Cause of apical thinning on attenuation-corrected myocardial perfusion SPECT

Nuclear Medicine Communications 2011: 32; 1033 - 1039
doi: 10.1097/MNM.0b013e32834b69e1

[Original article]

Cause of apical thinning on attenuation corrected myocardial perfusion SPECT

Koichi Okuda[1], Kenichi Nakajima[1, 2], Shinro Matsuo[2], Hiroshi Wakabayashi[2], Junichi Taki[2], Seigo Kinuya[1, 2]

1. Department of Nuclear Medicine, Faculty of Medicine, Institute of Medical, Pharmaceutical and Health Sciences, Kanazawa University, Kanazawa, Japan
2. Department of Nuclear Medicine, Kanazawa University Hospital, Kanazawa, Japan

Koichi Okuda, Ph.D.
Department of Nuclear Medicine, Faculty of Medicine, Institute of Medical, Pharmaceutical and Health Sciences, Kanazawa University
13-1 Takara-machi, Kanazawa, 920-8641, Japan
Tel +81-76 265 2333, Fax +81-76 234 4257,
E-mail: okuda@nmd.m.kanazawa-u.ac.jp

Secondary correspondence:
Kenichi Nakajima, MD, Ph.D.
Department of Nuclear Medicine, Kanazawa University Hospital
E-mail: nakajima@med.kanazawa-u.ac.jp

This work was supported in part by Grants-in-Aid for Scientific Research in Japan (No. 22591320, PI: Kenichi Nakajima)

Abstract

Objectives: Decreases in the apical and apex activities, namely “apical thinning”, are a well-known phenomenon in attenuation corrected (AC) myocardial perfusion. The aim of this study was to compare actual myocardial thickness derived from a multidetector-row computed tomography (MDCT) with AC myocardial perfusion count from a hybrid single-photon emission computed tomography (SPECT)/CT to investigate the cause of apical thinning.

Methods: We enrolled 21 subjects with low likelihood of coronary artery disease (mean age 65 ± 21 years, 13 male) from 185 consecutive patients and 11 healthy volunteers, who independently underwent Tc-99m sestamibi SPECT/CT and 64-slice MDCT scans. AC and non-AC myocardial perfusion counts and thickness were measured based on a 17-segment model and averaged at the apex, apical, mid and basal walls.

Results: Myocardial thickness at the apex was significantly thinner than that at the apical and mid walls (5.1 ± 1.3, 7.3 ± 1.3, 9.9 ± 2.4 mm, respectively, $p < 0.005$). AC count at the apex was significantly lower than that at the apical and mid regions (76.0 ± 5.5, 82.8 ± 4.7, 85.6 ± 3.8, respectively, $p < 0.002$). Moderate relationship was observed between myocardial thickness and AC count ($y = -10.5 + 0.22x$, $r = 0.54$, $p < 0.0001$). No relationship was found between thickness and non-AC count ($r = 0.16$, $p = 0.263$).

Conclusions: The low apex and apical counts were caused by anatomical thinning of the myocardium in AC myocardial perfusion imaging. AC provided accurate relationship between myocardial count and thickness due to the partial volume effect.

Key Words: apical thinning, attenuation correction, myocardial thickness, SPECT, MDCT, partial volume effect

Introduction

Myocardial perfusion imaging with single-photon emission computed tomography (SPECT) is the most widely used method for the assessment of patients with suspected or known coronary artery disease (CAD). Recently, since a hybrid SPECT/CT scanner can simultaneously provide myocardial perfusion SPECT (MPS) and computed tomography (CT) images, attenuation correction (AC) is sought after for reducing attenuation artifacts [1-12]. The diagnostic accuracy for the detection of CAD may be increased when MPS image is attenuation corrected using patient-specific non-uniform attenuation coefficient maps.

Attenuation correction, however, induces an artifactual myocardial perfusion defect at the apex, which is called “apical thinning” [11-14]. Subsequently, this phenomenon induces false-positive hypoperfusion in normal perfusion and reduces specificity for the detection of CAD. Apical thinning would attribute to partial volume effect due to myocardial thickness at the apex region and misregistration between MPS and CT. Although it has been extensively described on the effects of misregistration between MPS and CT in the apical regions [15-19], the relationship between AC myocardial perfusion count and thickness has not been clarified.

To investigate the cause of apical thinning, we assessed the relationship between AC myocardial perfusion counts and actual myocardial thickness derived from a multidetector-row CT (MDCT) in clinical subjects with normal MPS.

Methods

Study population

We retrospectively identified 185 consecutive patients and 11 healthy volunteers who underwent gated ^{99m}Tc-sestamibi (MIBI) MPS using a hybrid SPECT/CT between July 2008 and March 2011 in Kanazawa University Hospital. Exclusion criteria were history of coronary events, valvular heart disease, cardiomyopathy and chronic kidney disease. Furthermore, patients in whom motion error was observed in MPS scan were also excluded. Of this initial population, 45 subjects including 11 healthy volunteers were visually determined as a normal perfusion. Subsequently, 21 subjects underwent both MPS and MDCT scans in this group.

The final study group was consisted of 19 patients and 2 healthy volunteers. Median age of the patients was 73 years (range, 19 - 89 years). Stress and rest MPS imaging were performed at 40

minutes after injection of ^{99m}Tc MIBI of 300-370 MBq and 700-900 MBq, respectively. Pharmacologic (n=18) and exercise (n=1) stress tests were performed with an infusion of adenosine and bicycle exercise stress up to 100 Watt, respectively. Only rest test was performed in the 2 healthy volunteer. Table 1 summarizes subject characteristics. The institutional ethical committee approved the healthy volunteer study, and all volunteers gave informed consent.

Image acquisition

MPS scan was performed with a circular 360-degree acquisition with 60 projections at 35 seconds per projection by a dual-head gamma camera (Symbia T6, Siemens Japan, Tokyo, Japan) equipped with a low-energy high-resolution collimator. A pixel size was 6.6 mm for a 64 x 64 matrix. A photopeak window of ^{99m}Tc was set as a 15% energy window centered at 140 keV, and low sub-window for scatter correction was set 7%. Division of RR interval was 16 frames in gated acquisition. Gated and non-gated SPECT scans were performed using step-and-shoot acquisition. Low-dose CT image for AC was acquired with a 6-detector row CT on the hybrid SPECT/CT scanner. Mean tube voltage and current were 130 ± 0 kV and 72 ± 26 mA in low-dose CT scans, respectively. Gantry rotation time was set at 0.6 second. Axial images were reconstructed with a thickness of 5.0 mm. MDCT images for the measurement of myocardial thickness were acquired on the 64-MDCT scanner (LightSpeed VCT, GE Healthcare, Tokyo, Japan). Electrocardiographically (ECG)-gated coronary CT angiography (CCTA) was performed in 4 subjects, and non-ECG-gated standard helical chest scan was performed in 17 subjects. Iodinated contrast agent was intravenously injected. Mean tube voltage and current were 120 ± 0 kV and 921 ± 316 mA for ECG-gated CCTA, and 120 ± 0 kV and 168 ± 74 mA for non-ECG-gated scan.

Data analysis

AC short-axis images were reconstructed by ordered-subset expectation maximization (OSEM) with three-dimensional resolution recovery and scatter corrections using attenuation coefficient maps derived from the hybrid SPECT/CT scanner. Reconstruction parameters were set as 10 iterations and 10 subsets. A 13.2-mm Gaussian filter was applied to the reconstructed images. Non-AC (NC) short-axis images were reconstructed by filtered back projection (FBP) method with a Butterworth filter (cutoff, 0.68 Nyquist; order, 8). Resolution recovery and scatter corrections were not applied to NC images. Both reconstructions of AC and NC images were processed on e.soft workstation (Siemens Japan, Tokyo, Japan). After applying an automatic co-registration to

MPS and CT data sets [20], all sets were manually modified by the operator. AC and NC short-axis images were analyzed with quantitative perfusion SPECT (QPS) (version 2008) on the 17-segment model, and with which AC and NC normal databases were created. For the assessment of MDCT images, axial images were reconstructed with thicknesses of 0.63 mm (n = 11) and 1.25 mm (n= 10). Short-, horizontal long- and vertical long-axes images were reformatted from axial images. Myocardial thickness was manually measured with the reformatted images based on a 17-segment model. All measurements of myocardial thickness were performed on the dedicated workstation (Virtual Place Fujin, AZE Co., Ltd., Tokyo, Japan).

Statistical analysis

All continuous values were expressed as mean ± standard deviation (SD) unless otherwise noted. A paired t test was used to analyze the differences in paired continuous data. Tukey-Kramer method was also used to analyze the multiple comparison data. All statistical tests were two-tailed, and a p value of less than 0.05 was considered significant. The Pearson correlation analysis test was used for evaluating the relationship between myocardial perfusion count and thickness. These analyses were performed by using MedCalc software version 11.2.1.0 (Mariakerte, Belgium).

Results

The polar-map displays of mean AC MPS, NC MPS and myocardial thickness are shown in Fig. 1. Increases in the inferior and septal activities were visually observed in the AC normal database in comparison with the NC normal database, whereas decreases in the apex and anterior activities were also observed. Mean AC myocardial uptakes differed significantly at the anteroseptal, septal and inferior walls from NC myocardial uptakes in the quantitative assessment ($p < 0.016$). Myocardial thickness showed smallest value of 5.1 mm at the apex in the whole myocardium, and increased gradually toward to the basal myocardium.

Myocardial thickness in the apex, apical, mid and basal myocardiums are shown in Fig. 2. Myocardial thickness at the apex was significantly thinner than those at the apical, mid and basal regions (5.1 ± 1.3 mm for the apex, vs. 7.3 ± 1.3 mm for the apical region, $p = 0.0005$, vs. 9.9 ± 2.4 mm for the mid region, $p < 0.0001$, vs. 10.9 ± 2.1 mm for the basal region, $p < 0.0001$). Apical myocardial thickness was also significantly thinner than those at the mid and basal regions ($p = 0.0005$, < 0.0001, respectively). AC myocardial uptakes in the apex, apical, mid and basal

myocardiums are shown in Fig. 3. AC myocardial uptake at the apex demonstrated significant lower values than those at the apical and mid regions (76.0 ± 5.5 for the apex, vs. 82.8 ± 4.7 for the apical region, $p = 0.0002$, vs. 85.6 ± 3.8 for the mid region, $p < 0.0001$). Since the basal myocardial uptake indicated the edge of the myocardium and the aortic valve, lowest uptake was observed at the basal myocardium. NC myocardial uptakes in the apex, apical, mid and basal myocardiums are shown in Fig. 4. There were no significant differences among the apex, apical and mid regions.

The relationships between myocardial uptakes of AC and NC, and myocardial thickness at the apex, apical and mid regions are shown in Figs. 5 and 6. When the relationship between AC myocardial uptake (x) and thickness (y) was examined, moderate correlation was observed: $y = -10.5 + 0.22 x$, $r = 0.54$, $p < 0.0001$. However, there was no correlation between NC uptake and thickness ($r = 0.16$, $p = 0.263$).

An example of a patient with apical thinning is shown in Fig. 7. Apical thinning was visually observed in the polar map and horizontal long-axis image after AC. The thinning point at the left ventricular (LV) apex was measured as 4.4 mm on the MDCT image. Furthermore, the thickness and count of AC myocardium were corresponded better to that of MDCT image as compared with NC myocardium.

Discussion

We successfully observed and identified the moderate correlation between AC myocardial perfusion count and myocardial thickness in normal MPS subjects. In addition, both low AC myocardial uptake and myocardial thinning were recognized at the apex. Finally, “apical thinning” on the AC image may be caused by anatomical thinning of the myocardium. AC method would provide accurate relationship between myocardial count and thickness due to the partial volume effect.

Johnson et al. measured myocardial thickness of LV at the apex in 64 consecutive patients [21]. Myocardial thickness was less than 4.3 mm, and the average thickness was 1.2 mm. Frencik et al. also reported mean thickness of LV myocardium was 1.7 ± 0.7 mm in the apical thinnest point [22]. Our measurement showed slightly thicker myocardium in comparison with the previous reports. Grossman et al. studied AC normal databases of 22 female and 26 male subjects, which showed low apex activities of 82.7 ± 9.0 for female and 84.4 ± 8.8 for male as compared with 93.1 ± 7.1 and 94.8 ± 7.3 at the apical region, and 93.5 ± 7.8 and 92.9 ± 7.3 at the mid region, respectively [6]. Ficaro et al. also reported the characteristics of AC normal databases of 20 female

and 20 male subjects [12]. The 10 % to 15 % reduction was observed in the apex activity. In these previous studies, gender-composite AC normal database was created since no significant difference was observed between the AC female and male normal databases. Our gender-independent AC normal databases also showed no significant differences in excluding the basal anterior segment on a 17-segment model. Consequently, we created the gender-composite AC normal database and utilized this for the evaluation of this study. When the previous reported AC normal databases were compared with the present study, the characteristics of our AC normal database were visually and quantitatively similar.

Since a potential misregistration between MPS and CT images may occur in a hybrid SPECT/CT scanner [15-19], misregistration induced artifacts would possibly result in the cause of apical thinning. Matsunari et al. showed slight misregistration of a 7-mm shift (1 pixel) produced up to 15 % change in relatively regional uptake in the phantom study [15]. Misregistrations of more than 1 pixel were found 73 % of 248 consecutive MPS studies in the clinical study [18]. In addition, a 3-pixels misregistered shift significantly affected summed stress score for the detection of CAD. Nevertheless, misregistration induced artificial perfusions were simultaneously showed not only at the apex but also at the other regions. Then, the artificial perfusion would be different from apical thinning. In our study, since precise manual coregistration was applied after performing an automatic coregistration, AC MPS images would not generally be influenced by the misregistration.

When we utilized an AC in clinical patients and volunteers, SPECT scan was performed with a 360-degree acquisition. The 360-degree acquisition could improve both the homogeneity for myocardial count and image distortion in the deep part of the body. We will need further investigation on 180- and 360-degree SPECT acquisitions in the AC.

The partial volume effect is one of the physical phenomena in a nuclear medicine scan [23-25]. In our preliminary SPECT study for measuring the full width at half maximum (FWHM) of a line source, FWHM were 7.4 mm at the air after applying the resolution correction. On the other hand, the myocardial thickness was less than 10.9 mm, especially 5.1 mm at the apex, in our clinical measurements. In the current circumstance, the partial volume effect would be partially improved in the myocardial region, even if attenuation, scatter and resolution corrections are performed. Furthermore, since myocardial thickness at the apex is equivalent or less than a pixel size for an MPS acquisition, it is impossible to completely correct the partial volume effect in use of current technology.

The clinical implication of this study is that even in patients with normal myocardial perfusion, low apical activity is frequently observed after AC. The low uptake at the apex, however, is not an artifact caused by AC processing, but myocardial count is actually low based on the

physiological thinning of the myocardial apex. Therefore, quantitative assessment of AC MPS using normal AC databases may be helpful for the interpretation of low uptake at the apex. By using AC normal databases, diagnostic accuracy was significantly enhanced and misinterpretation in the apical region may be avoided [6, 10, 12].

Our study has several limitations. We did not have enough subjects for creating AC and NC normal databases and evaluating myocardial thickness. In addition, AC and NC normal databases were individually constructed with the different reconstruction methods of OSEM and FBP, respectively. Kovalski et al. reported OSEM with resolution correction emphasized myocardial perfusion artifact due to respiratory-related cardiac motion [26]. When we evaluated AC and NC normal databases, gender-related normal databases were not utilized. In our preliminary study, a segmental difference of gender-related NC normal databases was observed only at the mid inferior on 17-segment model ($p = 0.036$). Furthermore, we did not have enough subjects to compare the gender-related NC normal databases. Consequently, we combined female and male NC normal databases. As for the AC normal database, no segmental difference was observed between female and male except for the basal anterior region. For the acquisition of MDCT data, ECG-gated CCTA was performed in a part of the subjects. Thus, the mean myocardial thickness at the apex was slightly larger than that from the previously reported data. When we apply ECG-gated CCTA acquisition to all the patients, a mean myocardial thickness would be decreased, and relationship between AC myocardial perfusion count and thickness may be improved.

Conclusion

The results of our study indicate that the cause of apical thinning on AC MPS is related to an anatomical thinning of the myocardium. AC MPS is strongly affected by the anatomical characteristics of the myocardium.

Acknowledgement

We thank Masato Yamada, RT, Minoru Tobisaka, RT, Shigeto Matsuyama, RT, Keita Sakuta, RT (Kanazawa University Hospital, Kanazawa, Japan) and Hiroyuki Arai (Siemens Japan, Tokyo, Japan) for their technological assistance. We also thank Masahiro Kubota (Toshiba Medical Systems Corporation, Tokyo, Japan) for help with study design. The authors declare no conflict of

interests. This work was supported in part by Grants-in-Aid for Scientific Research in Japan (No. 22591320, PI: Kenichi Nakajima).

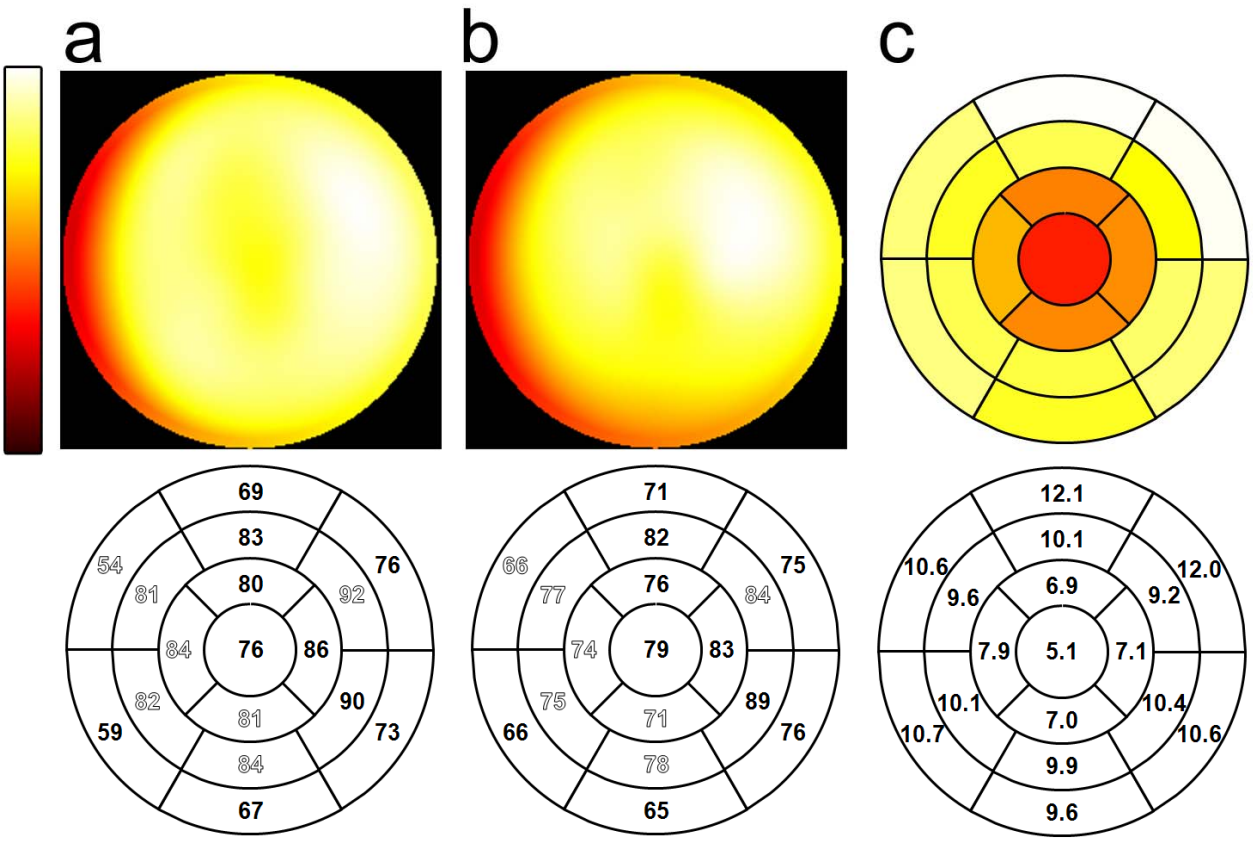

Fig. 1. Polar-map displays of mean normal AC (a) and NC (b) myocardial perfusion databases and thickness distribution (c) derived from 19 patients with normal perfusion and 2 healthy volunteers. Outline fonts denote significant differences between AC and NC databases ($p < 0.02$). Segmental values are expressed in millimeters on the polar map of myocardial thickness.

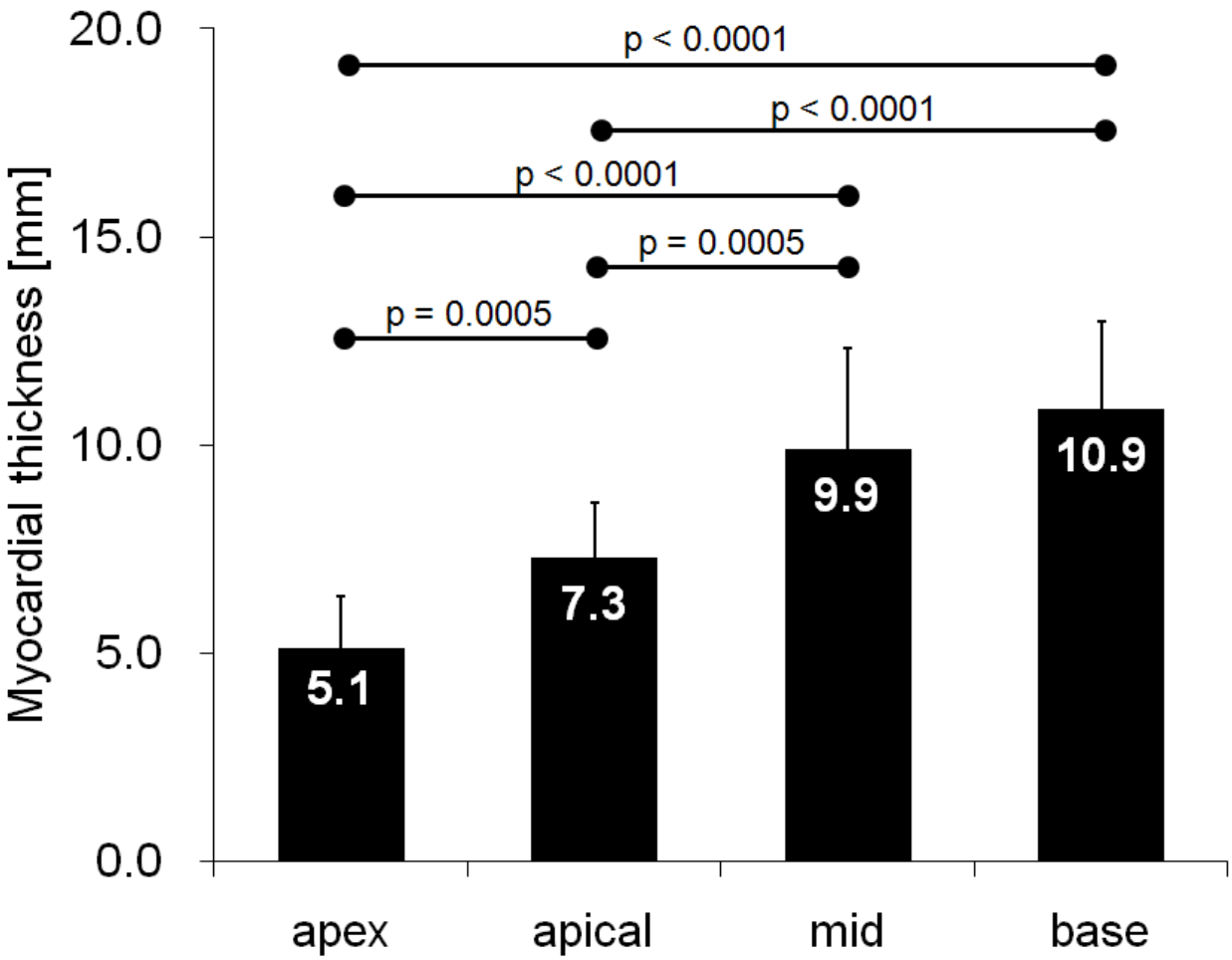

Fig. 2. Averaged myocardial thickness in the apex, apical, mid and basal regions.

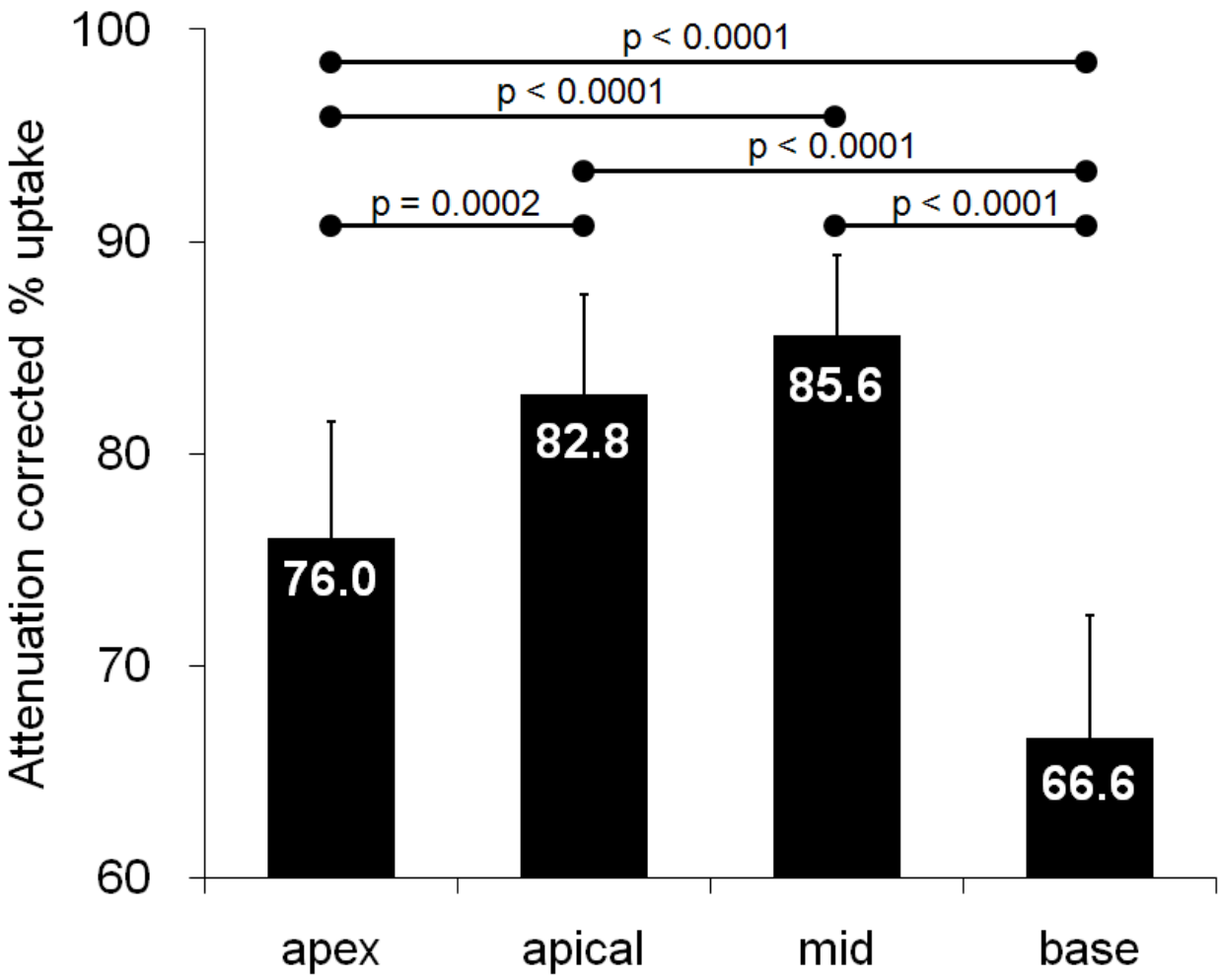

Fig. 3. Averaged AC myocardial counts in the apex, apical, mid and basal regions.

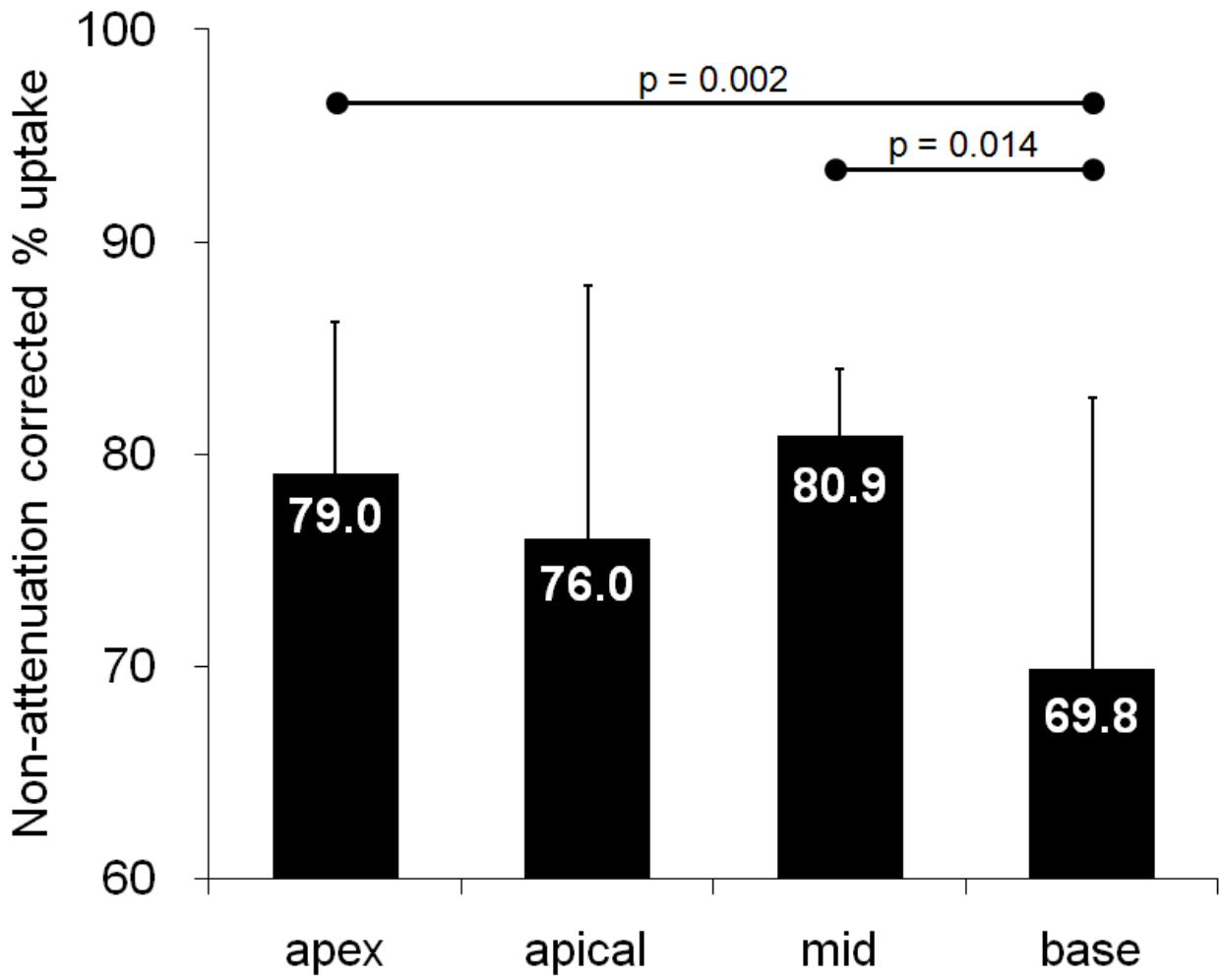

Fig. 4. Averaged NC myocardial counts in the apex, apical, mid and basal regions.

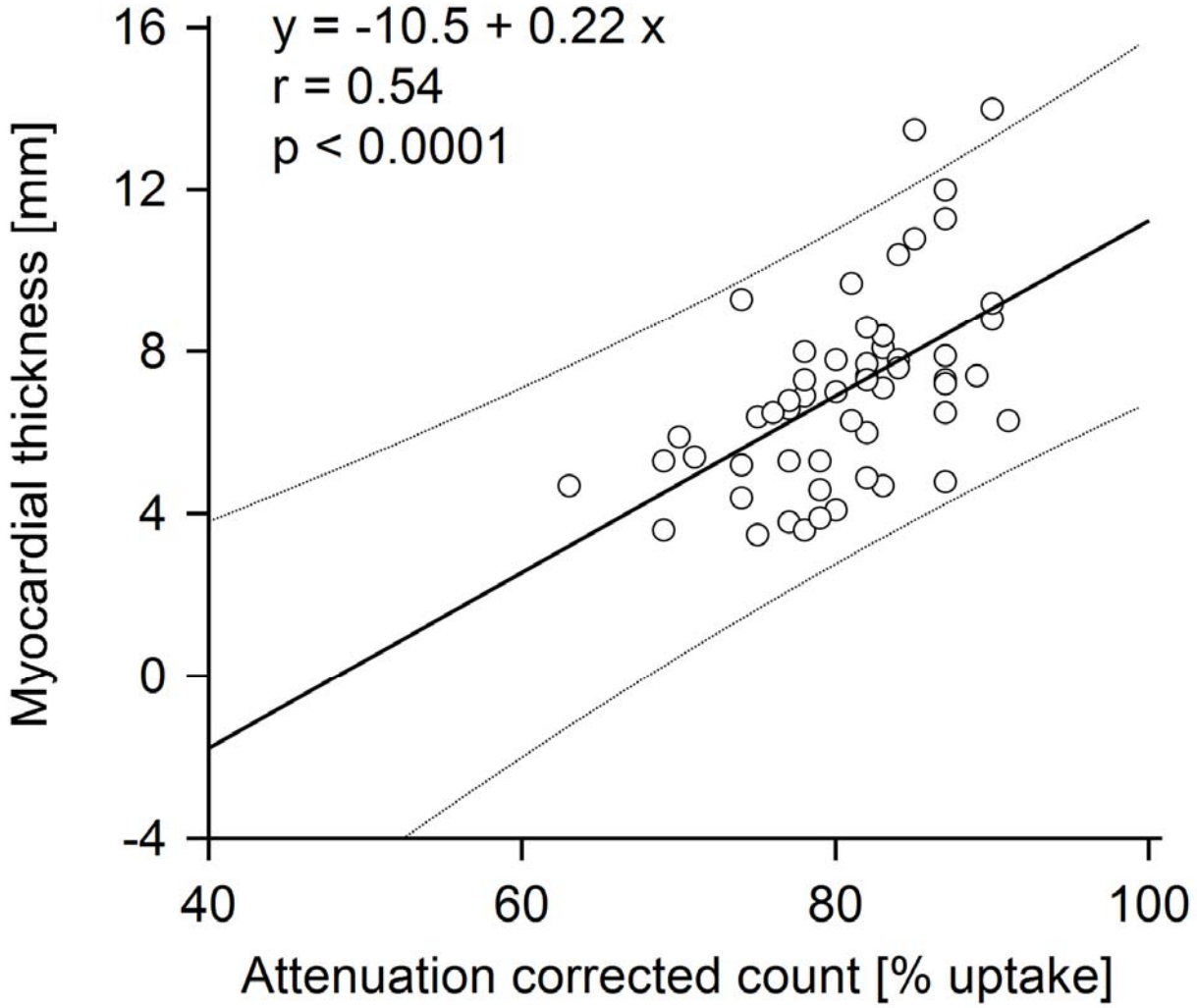

Fig. 5. Relationship between AC myocardial count and myocardial thickness. Dotted lines denote upper and lower limits of the 95% prediction interval.

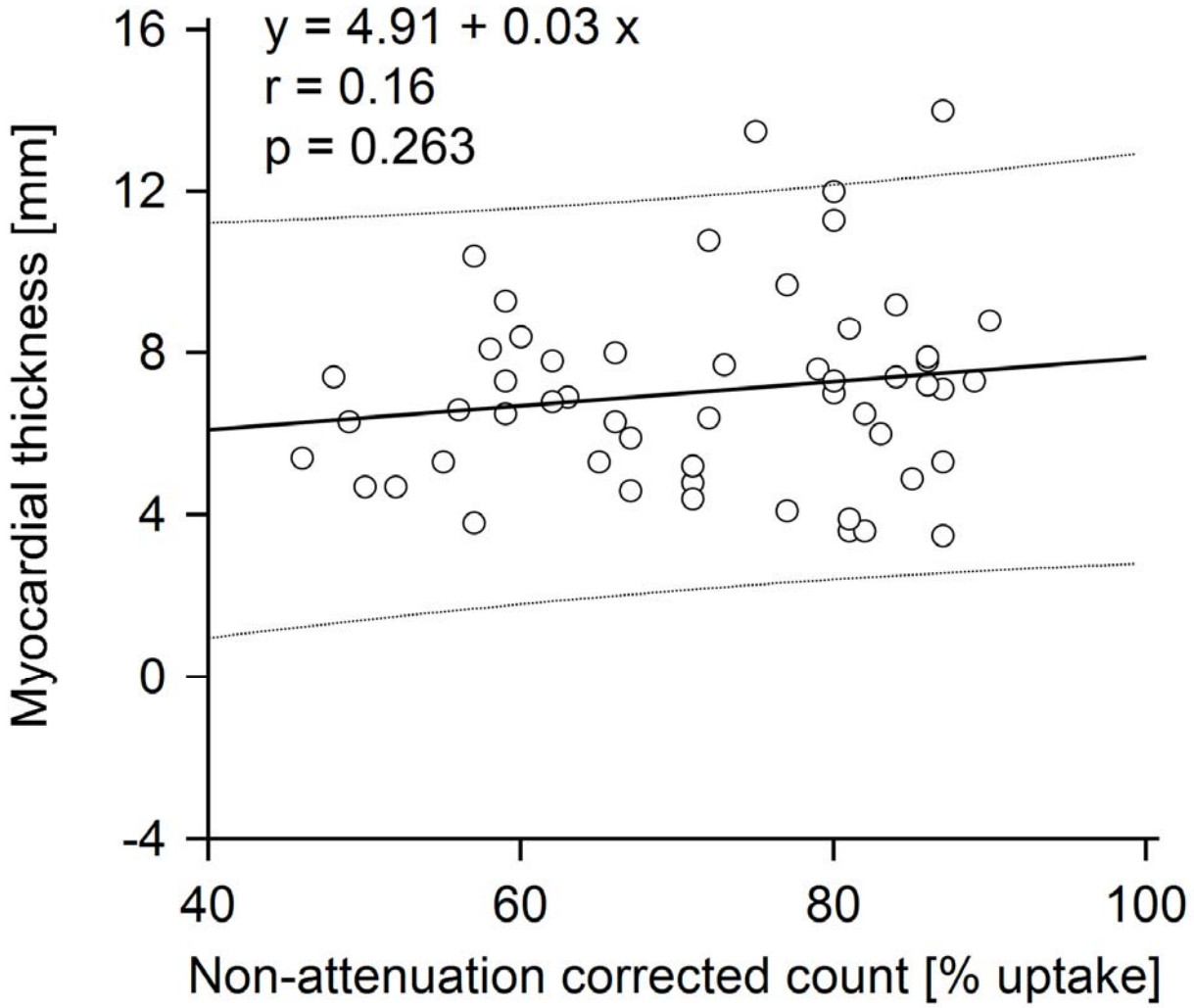

Fig. 6. Relationship between NC myocardial count and myocardial thickness.

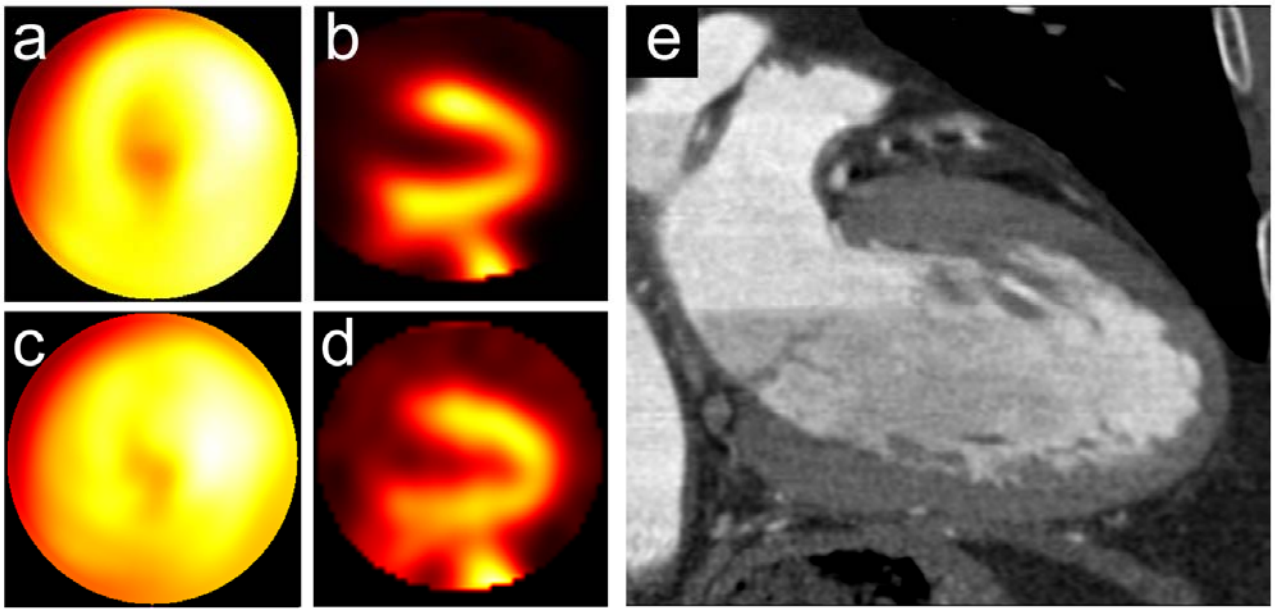

Fig. 7. An example of apical thinning in a 72-year-old male patient with BMI of 22 kg/m^2. EF, EDV and ESV were 68 %, 71 ml and 23 ml, respectively. Apical thinning was clearly observed in the AC polar map and horizontal long-axis view (a, b) in comparison with NC polar map and horizontal long-axis view (c, d). On a reformatted horizontal long-axis view of MDCT image (e), myocardial thinning was also observed at the left ventricular apex.

Table 1. Characteristics of subjects

Parameter	Value
Total	21
Female / Male	8 / 13
Age	65.0 ± 20.9
Height (m)	1.60 ± 0.09
Weight (kg)	55 ± 11
BMI (kg/m^2)	21.4 ± 3.3
Hypertension	2 (9.5%)
Hypercholesterolemia	2 (9.5%)
Diabetes	1 (4.8%)
gated SPECT data	
LVEF (%)	73.2 ± 10.4
EDV (mL)	59.2 ± 16.5
ESV (mL)	16.8 ± 8.9

BMI body Mass Index, *LVEF* left ventricular ejection fraction, *EDV* end-diastolic volume, *ESV* end-systolic volume.

References

1. Flotats A, Knuuti J, Gutberlet M, Marcassa C, Bengel FM, Kaufmann PA, et al. Hybrid cardiac imaging: SPECT/CT and PET/CT. A joint position statement by the European Association of Nuclear Medicine (EANM), the European Society of Cardiac Radiology (ESCR) and the European Council of Nuclear Cardiology (ECNC). Eur J Nucl Med Mol Imaging. 2011;38:201-12.

2. Hendel RC, Berman DS, Cullom SJ, Follansbee W, Heller GV, Kiat H, et al. Multicenter clinical trial to evaluate the efficacy of correction for photon attenuation and scatter in SPECT myocardial perfusion imaging. Circulation. 1999;99:2742-9.

3. Heller GV, Links J, Bateman TM, Ziffer JA, Ficaro E, Cohen MC, et al. American Society of Nuclear Cardiology and Society of Nuclear Medicine joint position statement: attenuation correction of myocardial perfusion SPECT scintigraphy. J Nucl Cardiol. 2004;11:229-30.

4. Apostolopoulos DJ, Spyridonidis T, Skouras T, Giannakenas C, Savvopoulos C, Vassilakos PJ. Comparison between 180 degrees and 360 degrees acquisition arcs with and without correction by CT-based attenuation maps in normal hearts at rest. Nucl Med Commun. 2008;29:110-9.

5. Kojima A, Tomiguchi S, Kawanaka K, Utsunomiya D, Shiraishi S, Nakaura T, et al. Attenuation correction using asymmetric fanbeam transmission CT on two-head SPECT system. Ann Nucl Med. 2004;18:315-22.

6. Grossman GB, Garcia EV, Bateman TM, Heller GV, Johnson LL, Folks RD, et al. Quantitative Tc-99m sestamibi attenuation-corrected SPECT: development and multicenter trial validation of myocardial perfusion stress gender-independent normal database in an obese population. J Nucl Cardiol. 2004;11:263-72.

7. Utsunomiya D, Tomiguchi S, Shiraishi S, Yamada K, Honda T, Kawanaka K, et al. Initial experience with X-ray CT based attenuation correction in myocardial perfusion SPECT imaging using a combined SPECT/CT system. Ann Nucl Med. 2005;19:485-9.

8. Taneja S, Mohan HK, Blake GM, Livieratos L, Clarke SE. Synergistic impact of attenuation correction and gating in routine myocardial SPECT reporting: 2 year follow-up study. Nucl Med Commun. 2008;29:390-7.

9. Okuda K, Nakajima K, Motomura N, Kubota M, Yamaki N, Maeda H, et al. Attenuation correction of myocardial SPECT by scatter-photopeak window method in normal subjects. Ann Nucl Med. 2009;23:501-6.

10. Xu Y, Fish M, Gerlach J, Lemley M, Berman DS, Germano G, et al. Combined quantitative analysis of attenuation corrected and non-corrected myocardial perfusion SPECT: Method development and clinical validation. J Nucl Cardiol. 2010;17:591-9.

11. Wakabayashi Y, Imai K, Morozumi K, Takahashi Y, Shibasaki M. Evaluation of Tc-99m-myocardial perfusion SPECT attenuation correction by hybrid SPECT/CT-examination by quantitative analysis. Nippon Hoshasen Gijutsu Gakkai Zasshi. 2010;66:371-8.

12. Ficaro EP, Fessler JA, Shreve PD, Kritzman JN, Rose PA, Corbett JR. Simultaneous transmission/emission myocardial perfusion tomography. Diagnostic accuracy of attenuation-corrected 99mTc-sestamibi single-photon emission computed tomography. Circulation. 1996;93:463-73.

13. Purser NJ, Armstrong IS, Williams HA, Tonge CM, Lawson RS. Apical thinning: real or artefact? Nucl Med Commun. 2008;29:382-9.

14. Links JM, Becker LC, Anstett F. Clinical significance of apical thinning after attenuation correction. J Nucl Cardiol. 2004;11:26-31.

15. Matsunari I, Boning G, Ziegler SI, Kosa I, Nekolla SG, Ficaro EP, et al. Effects of misalignment between transmission and emission scans on attenuation-corrected cardiac SPECT. J Nucl Med. 1998;39:411-6.

16. Takahashi Y, Murase K, Higashino H, Mochizuki T, Motomura N. Attenuation correction of myocardial SPECT images with X-ray CT: effects of registration errors between X-ray CT and SPECT. Ann Nucl Med. 2002;16:431-5.

17. Goetze S, Brown TL, Lavely WC, Zhang Z, Bengel FM. Attenuation correction in myocardial perfusion SPECT/CT: effects of misregistration and value of reregistration. J Nucl Med. 2007;48:1090-5.

18. Kennedy JA, Israel O, Frenkel A. Directions and magnitudes of misregistration of CT attenuation-corrected myocardial perfusion studies: incidence, impact on image quality, and guidance for reregistration. J Nucl Med. 2009;50:1471-8.

19. Tonge CM, Ellul G, Pandit M, Lawson RS, Shields RA, Arumugam P, et al. The value of registration correction in the attenuation correction of myocardial SPECT studies using low resolution computed tomography images. Nucl Med Commun. 2006;27:843-52.

20. Maes F, Collignon A, Vandermeulen D, Marchal G, Suetens P. Multimodality image registration by maximization of mutual information. IEEE Trans Med Imaging. 1997;16:187-98.

21. Johnson KM, Johnson HE, Dowe DA. Left ventricular apical thinning as normal anatomy. J Comput Assist Tomogr. 2009;33:334-7.

22. Ferencik M, Abbara S, Hoffmann U, Cury RC, Brady TJ, Achenbach S. Left ventricular thin-point detection using multidetector spiral computed tomography. Am J Cardiol. 2004;93:949-51.

23. Motomura N, Nambu K, Kojima A, Tomiguchi S, Ogawa K. Development of a collimator

blurring compensation method using fine angular sampling projection data in SPECT. Ann Nucl Med. 2006;20:337-40.

24. Pretorius PH, King MA. Diminishing the impact of the partial volume effect in cardiac SPECT perfusion imaging. Med Phys. 2009;36:105-15.

25. Watson DD. Quantitative SPECT techniques. Semin Nucl Med. 1999;29:192-203.

26. Kovalski G, Keidar Z, Frenkel A, Israel O, Azhari H. Correction for respiration artefacts in myocardial perfusion SPECT is more effective when reconstructions supporting collimator detector response compensation are applied. J Nucl Cardiol. 2009;16:949-55.